



Light Curve and Period Change Behavior of a Binary Star V392 Orionis

Wiraporn Maithong^{1*}, Torik Hengpiya², and Chaloemchon Wannathong³

¹ Faculty of Science and Technology, Chiang Mai Rajabhat University, Chiang Mai, 50300, Thailand

² National Astronomical Research Institute of Thailand (Public Organization), Songkhla, 90000, Thailand

³ Faculty of Science Technology and Agriculture, Yala Rajabhat University, Yala, 95000, Thailand

* Correspondence: wiraporn_mai@cmru.ac.th

Abstract: This study investigates the period change of the eclipsing binary system V392 Orionis (V392 Ori), which is classified as an Algol-type binary star. The research utilized data from the TESS Eclipsing Binary Catalog obtained via the Transiting Exoplanet Survey Satellite (TESS). Light curves were generated through photometric analysis to determine the times of minimum light. The historical and current observational data were used to construct the O-C diagram. The O-C diagram derived from PE and CCD observations exhibits a downward parabolic trend, indicating a decreasing orbital period at a rate of 5.76×10^{-3} seconds per year.

Citation:

Maithong, W.; Hengpiya, T.; Wannathong, C. Light curve and period change behavior of a binary star V392 orionis. *ASEAN J. Sci. Tech. Report.* **2025**, *28*(5), e259078. <https://doi.org/10.55164/ajstr.v28i5.259078>.

Article history:

Received: April 30, 2025

Revised: August 18, 2025

Accepted: September 1, 2025

Available online: September 14, 2025

Publisher's Note:

This article is published and distributed under the terms of the Thaksin University.

Keywords: V392 Ori; Period Change; O-C Diagram

1. Introduction

Binary systems are stellar systems composed of two stars orbiting a common center of mass under mutual gravitational attraction [1]. The study of binary star systems allows astronomers to determine the physical properties of stars and understand stellar evolution [2]. The binary star systems can be classified into two major types: visual binary systems, where individual stars can be distinguished through a telescope, and close binary systems, where the components are so close that they appear as a single star and can only be identified as binaries through other analytical methods. The type of a binary system is typically classified by constructing a light curve, which plots the variation in brightness over time. A dip in the light curve indicates an eclipse event where one star blocks the other along the observer's line of sight. In a whole orbital period of a binary system, two eclipses typically occur, corresponding to the primary and secondary eclipses. The time it takes for the system to complete one full orbit is referred to as the orbital period.

V392 Orionis (V392 Ori) is an Algol-type close eclipsing binary star with a spectral type of A5V. Its celestial coordinates are RA 06h 11m 25.17s and Dec $+18^{\circ} 32' 59.60''$. [3] The orbital period is 0.659284 days [4] and decreasing. [5] This study aims to analyze the period change of V392 Ori through its O-C diagram, contributing to a better understanding of the system's long-term behavior and evolution.

2. Materials and Methods

The study of the light variation of the binary star V392 Ori involved data collected from the TESS Eclipsing Binary Catalog, which contains observations

from the Transiting Exoplanet Survey Satellite (TESS). The TESS, operated by NASA, is accessible via the website <http://tessebs.villanova.edu> [6]. The TESS conducts observations of exoplanets, variable stars, and binary star systems, collecting data within the wavelength range of 600–1,000 nanometers, which corresponds to portions of the R to I bands in the Johnson UBV photometric system, as illustrated in Figure 1. [7]

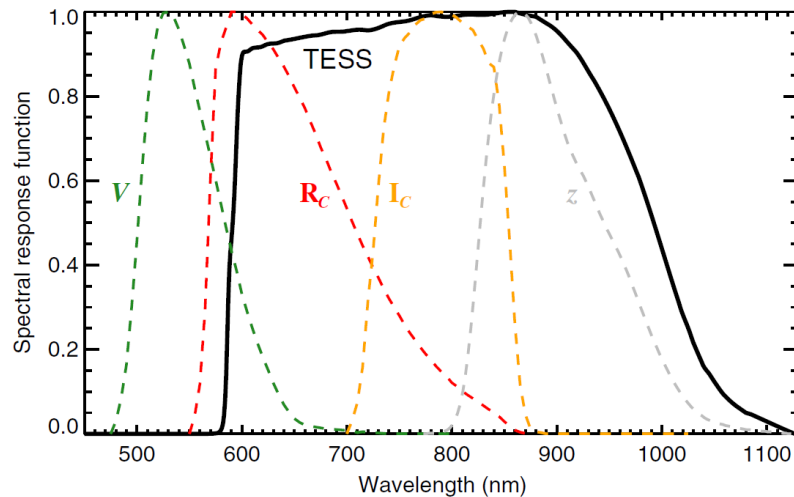


Figure 1. The black line is the wavelength bandwidth of the TESS observation.

This work uses Python code to download the data of V392 Ori, including the BJD time of observation and flux. The data at the latest time were used to plot the light curve as illustrated in Figure 2.

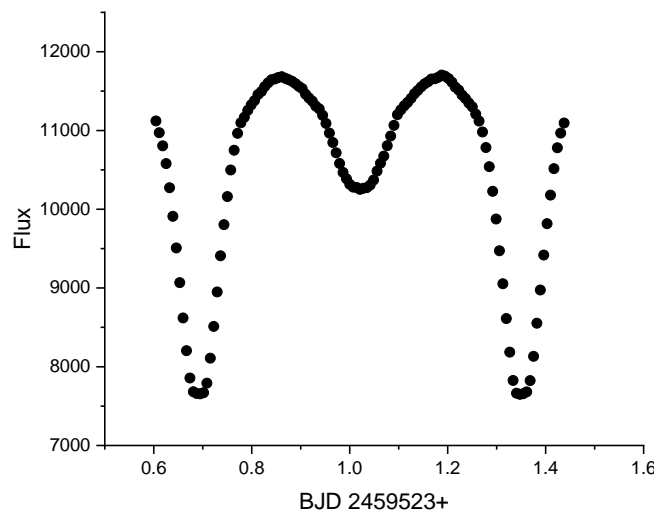


Figure 2. The light curve of V392 Ori, plotted from TESS observational data.

3. Results and Discussion

In Figure 2, the vertical axis represents the flux, and the horizontal axis represents time in Barycentric Julian Date (BJD), a time standard that accounts for the motion of light and other relevant factors by referencing the barycenter of the solar system. From this light curve, the times of minimum light were determined by fitting parabolic curves to the regions around the minima. The minimum time obtained in this study is BJD 2459523.691. The period change analysis was conducted following the procedure described by

Bob Nelson [8], as referenced by the American Association of Variable Star Observers (AAVSO), where the Heliocentric Julian Date (HJD) is converted to Barycentric Julian Date (BJD). The linear ephemeris used in this study is:

$$\text{Min. I} = \text{BJD } 2425506.620 + 0.659284 \text{ E} \quad (1)$$

Where: Min. I = BJD time of primary minimum

E = Epoch (number of orbital cycles since the initial reference time)

The O–C values of the eclipsing binary system V392 Ori, based on the times of minimum compiled by Bob Nelson [8], were computed from equation (1) as shown in Table 1.

Table 1. O–C values for the eclipsing binary system V392 Ori

Time of Minimum BJD	Epoch	O–C	Photograph	Source
2425506.62	0	0	pg	GCVS 4
2425506.624	0	0.004	pg	MVS 3.199
2426224.583	1089	0.002724	pg	MVS 3.199
2426743.425	1876	-0.011784	pg	MVS 3.199
2428453.629	4470	0.00952	pg	VSS 2.56
2428494.467	4532	-0.028088	pg	VSS 2.56
2428547.276	4612	0.038192	pg	VSS 2.56
2428809.597	5010	-0.03584	pg	VSS 2.56
2429167.598	5553	-0.026052	pg	VSS 2.56
2429229.567	5647	-0.029748	pg	VSS 2.56
2429231.59	5650	0.0154	pg	VSS 2.56
2429251.35	5680	-0.00312	pg	VSS 2.56
2429340.354	5815	-0.00246	pg	VSS 2.56
2429630.469	6255	0.02758	pg	VSS 2.56
2429641.317	6271.5	-0.002606	pg	VSS 2.56
2429729.328	6405	-0.00602	pg	VSS 2.56
2429943.596	6730	-0.00532	pg	VSS 2.56
2429957.471	6751	0.024716	pg	VSS 2.56
2430326.609	7311	-0.036324	pg	VSS 2.56
2430375.422	7385	-0.01034	pg	VSS 2.56
2430778.27	7996	0.015136	pg	MVS 3.199
2432118.601	10029	0.021764	pg	MVS 3.199
2432908.4	11227	-0.001468	pg	MVS 3.199
2433186.588	11649	-0.031316	pg	MVS 3.199
2433357.358	11908	-0.015872	pg	VSS 2.56
2433361.332	11914	0.002424	pg	MVS 3.199
2433378.15	11939.5	0.008682	pg	AC 151.26
2433597.32	12272	-0.033248	pg	AC 151.26
2433630.3	12322	-0.017448	pg	AC 151.26
2433659.29	12366	-0.035944	pg	AC 151.26
2434088.15	13016.5	-0.040186	pg	AC 151.26
2434420.12	13520	-0.01968	pg	AC 151.26
2434653.544	13874	0.017784	pg	MVS 3.199
2435135.41	14605	-0.05282	pg	MVS 3.199
2435164.446	14649	-0.025316	pg	MVS 3.199
2435892.339	15753	0.018148	pg	MVS 3.199

2435921.352	15797	0.022652	pg	MVS 3.199
2436604.322	16833	-0.025572	pg	MVS 3.199
2436608.28	16839	-0.023276	pg	MVS 3.199
2436896.412	17276	0.001616	pg	HABZ 98
2437312.418	17907	-0.000588	pg	MVS 644
2437345.369	17957	-0.013788	pg	HABZ 98
2437349.36	17963	0.021508	pg	HABZ 98
2437917.624	18825	-0.0173	pg	MVS 3.199
2438088.397	19084	0.001144	pg	HABZ 98
2438372.526	19515	-0.02126	pg	MVS 3.199
2438411.458	19574	0.012984	pg	MVS 3.199
2438440.458	19618	0.004488	pg	HABZ 98
2438670.58	19967	0.036372	pg	MVS 3.199
2439024.547	20504	-0.032136	pg	MVS 3.199
2439055.556	20551	-0.009484	pg	MVS 3.199
2439057.581	20554	0.037664	pg	MVS 3.199
2439059.517	20557	-0.004188	pg	HABZ 98
2439088.545	20601	0.015316	pg	MVS 3.199
2439528.276	21268	0.003888	pg	HABZ 98
2440981.332	23472	-0.002048	pg	HABZ 98
2441329.444	24000	0.007	pg	HABZ 98
2441331.416	24003	0.001148	pg	HABZ 98
2441333.394	24006	0.001296	pg	HABZ 98
2442404.725	25631	-0.004204	pg	BBS 19
2442417.28	25650	0.0244	pg	BBS 20
2442475.28	25738	0.007408	pg	HABZ 98
2443212.368	26856	0.015896	pg	BBS 33
2445052.421	29647	0.007252	pg	VSSC 60.22
2445054.398	29650	0.0064	pg	VSSC 60.22
2447231.361	32952	0.013632	vis	BBS 88
2447233.331	32955	0.00578	vis	BBS 88
2447554.39	33442	-0.006528	vis	BBS 91
2447564.282	33457	-0.003788	vis	BBS 91
2447566.28	33460	0.01636	vis	BAVM 52
2447587.367	33492	0.006272	vis	BBS 91
2447914.367	33988	0.001408	vis	BBS 94
2447922.308	34000	0.031	vis	BBS 94
2447941.423	34029	0.026764	vis	BBS 94
2447943.419	34032	0.044912	vis	BBS 94
2448272.361	34531	0.004296	vis	IBVS 4097
2448272.364	34531	0.006996	vis	IBVS 4097
2448307.308	34584	0.009144	vis	BBS 97
2448332.352	34622	0.000352	vis	BBS 97
2448688.365	35162	-8E-06	vis	BBS 101
2450390.627	37744	-0.009296	vis	BBS 116
2450483.597	37885	0.00126	PE	BBS 114
2451925.451	40072	0.001652	PE	IBVS 5296
2452647.368	41167	0.002772	PE	IBVS 5643
2452654.622	41178	0.004348	CCD	IBVS 5502
2452655.278	41179	0.000964	CCD	IBVS 5438

2452715.274	41270	0.00182	CCD	IBVS 5676
2452998.766	41700	0.002	CCD	IBVS 5493
2453354.121	42239	0.002724	CCD	VSB 43
2453450.376	42385	0.00286	CCD	IBVS 5741
2453671.897	42721	0.003936	CCD	IBVS 5677
2453674.535	42725	0.0048	CCD	IBVS 5741
2453696.291	42758	0.004228	CCD	VSB 44
2453700.246	42764	0.003924	CCD	VSB 44
2453715.41	42787	0.004592	CCD	IBVS 5741
2453758.261	42852	0.001632	PE	IBVS 5802
2454068.788	43323	0.006268	CCD	IBVS 5760
2454091.534	43357.5	0.00667	PE	IBVS 5761
2454476.553	43941.5	0.003614	PE	IBVS 5874
2454521.382	44009.5	0.001652	CCD	OEJV 0094
2454809.161	44446	0.003436	CCD	VSB 48
2454829.599	44477	0.003232	PE	IBVS 5918
2454881.684	44556	0.004996	CCD	IBVS 5894
2455135.177	44940.5	0.003798	CCD	VSB 50
2455136.165	44942	0.002172	CCD	VSB 50
2455158.913	44976.5	0.004974	CCD	IBVS 5920
2455163.854	44984	0.001544	CCD	IBVS 5929
2455244.287	45106	0.001796	PE	IBVS 5959
2455591.73	45633	0.002128	CCD	IBVS 5992
2455602.278	45649	0.001684	PE	IBVS 6070
2455838.629	46007.5	-0.00063	CCD	OEJV 0142
2456256.945	46642	-0.000828	CCD	IBVS 6042
2457042.487	47833.5	0.004586	PE	IBVS 6152
2457296.632	48219	-0.004196	CCD	IBVS 6230
2457414.308	48397.5	-0.01029	CCD	IBVS 6196
2457702.091	48834	-0.004556	CCD	VSB-063
2458058.105	49374	-0.004416	CCD	VSB-64
2458219.63	49619	-0.004178	CCD	JAVSO 49, 106
2458785.954	50478	-0.005088528	CCD	RHN 2019
2459523.691	51597	-0.0052129	CCD	This Study
2459938.063	52225.5	0.005658	CCD	VSB, 108

Note:

pg (photographic): Refers to observations derived from astronomical photographic plates or films, which were commonly used in early stellar photometry.

vis (visual): Refers to visually estimated observations, obtained either with the unaided eye or through a telescope. The timing of events is subject to the observer's judgment and experience.

PE (photoelectric): Refers to measurements acquired using a photoelectric photometer, a method prevalent before the development of CCD technology. This technique provided improved accuracy over visual methods.

CCD (Charge-Coupled Device): Refers to observations obtained using CCD sensors, a modern and highly precise technique in photometric measurements that has become the standard in contemporary astronomical research. The O-C values derived from the observed times of minimum light (O) and the predicted times (C) were plotted against the corresponding epochs to produce the O-C diagram. This study considers the period change in three solutions: the first is computed from all data, the second calculates from vis to present, and the last one analyzes especially PE and CCD. The first solution is the O-C diagram of V392 Ori, as shown in Figure 3.

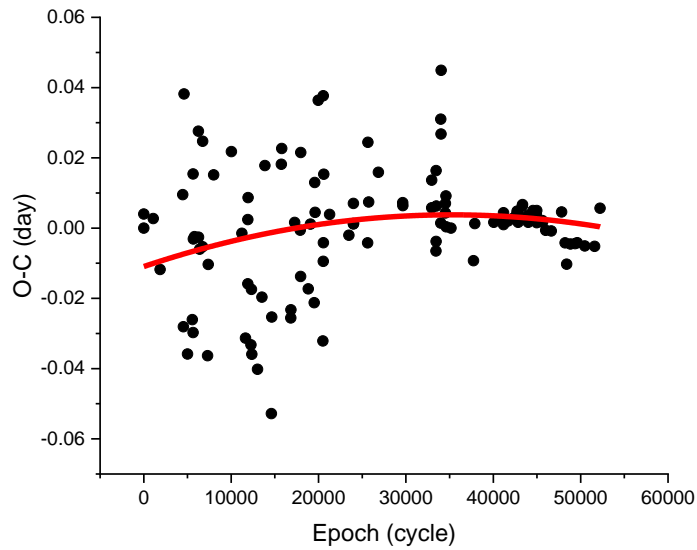


Figure 3. The O-C diagram for V392 Ori, based on all available data.

The parabolic nature of the O-C diagram indicates a trend of increasing orbital period. A second-order polynomial fit was applied using the Quadratic Polynomial Fitting Method, resulting in the following equation:

$$O-C = -0.01094 + 8.35174 \times 10^{-7} \text{ Epoch} - 1.18474 \times 10^{-11} \text{ Epoch}^2 \quad (2)$$

From this, the rate of orbital period change (dP/dE) can be calculated as:

$$\begin{aligned} dP/dE &= 2(-1.18474 \times 10^{-11}) \\ &= -2.3694 \times 10^{-11} \text{ day/cycle} \\ &= -1.134 \times 10^{-3} \text{ sec/year} \end{aligned}$$

This negative value of dP/dE indicates that the orbital period of the binary system V392 Ori is decreasing. This suggests that the distance between the two stellar components is decreasing, consistent with the Angular Momentum Loss (AML) theory [9]. The loss of angular momentum in a binary star system drives orbital evolution, which may ultimately result in the merger of the two components into a single, rapidly rotating star. The second solution, the O-C diagram of V392 Ori, was computed from data except for pg , as shown in Figure 4.

The O-C diagram from Figure 4 shows that there is a periodic pattern (blue line) on the second-order polynomial line (red line). The second-order polynomial and sinusoidal fit to the O-C data yielded the following equation:

$$\begin{aligned} O-C &= 0.05561 - 1.7805 \times 10^{-6} \text{ Epoch} + 1.2656 \times 10^{-11} \text{ Epoch}^2 \\ &\quad + -0.00145 + 0.00349 \sin(\pi((\text{Epoch} - 1447.9893)/4972.98766)) \end{aligned} \quad (3)$$

So,

$$\begin{aligned} dP/dE &= 2 \times 1.2656 \times 10^{-11} \\ &= 2.5312 \times 10^{-11} \text{ day/cycle} \\ &= 1.21 \times 10^{-3} \text{ sec/year} \end{aligned}$$

The positive rate of change of the period (1.21×10^{-3} seconds/year) suggests that the orbital separation between the two stars is increasing. This supports the Thermal Relaxation Oscillation (TRO) theory [10], which

suggests that variations in the internal structure and energy balance of the components, combined with mass transfer between them, can drive cyclic changes between contact and semi-detached configurations, thereby influencing the orbital evolution of the system. This periodic variation indicates the likely presence of a third body in the system. The light-time effect gives an orbital radius of approximately 0.67 AU for the third body, with an orbital period of about 17.95 years. The third solution, the O-C diagram of the V392 Ori, was calculated from PE and CCD data as shown in Figure 5.

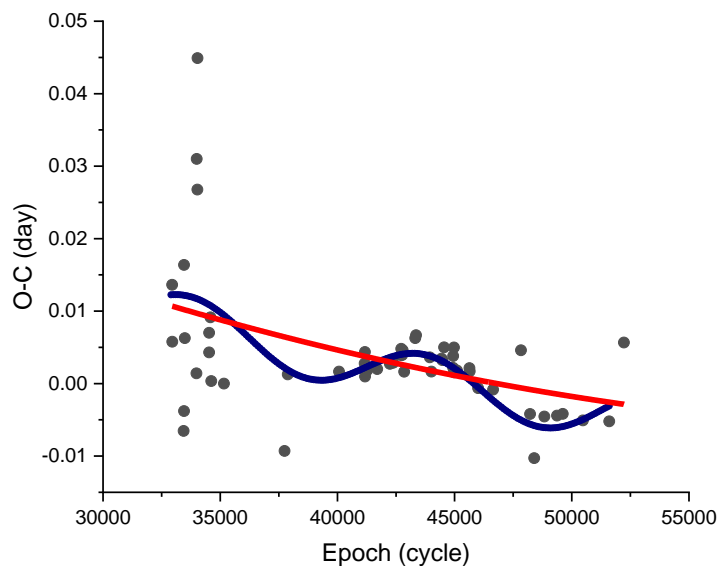


Figure 4. The O-C diagram for the V392 Ori from vis to present data.

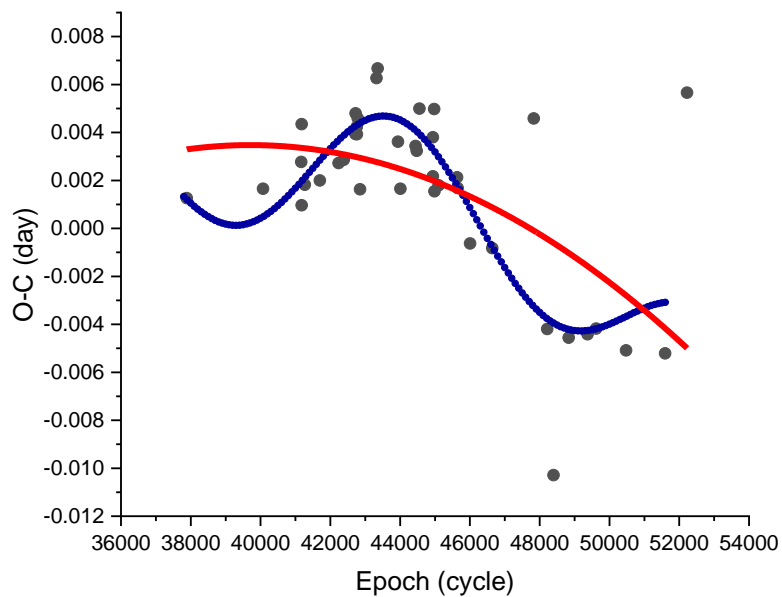


Figure 5. The O-C diagram for V392 Ori, based on PE and CCD data.

The O-C diagram from Figure 5 exhibits a similar pattern to that in Figure 3, which is a periodic pattern (blue line) on the second-order polynomial line (red line). Therefore, the O-C data yielded the following equation:

$$\begin{aligned} \text{O-C} &= -0.08178 + 4.29419 \times 10^{-6} \text{ Epoch} - 5.40715 \times 10^{-11} \text{ Epoch}^2 \\ &\quad -0.000642856 + 0.0027 \sin(\pi((\text{Epoch} - 23541.55743) / 4510.50998)) \end{aligned} \quad (4)$$

So,

$$\frac{dP}{dE} = -5.176 \times 10^{-3} \text{ sec/year}$$

The negative rate of change of the period (-5.176×10^{-3} seconds/year) is consistent with the evolution of AML theory. The sinusoidal variation may indicate the presence of a third body in this system, which is positioned approximately 0.47 AU from the primary body and has an approximate orbital period of 16.28 years.

4. Conclusions

This study of the eclipsing binary system V392 Ori used data from the TESS Eclipsing Binary Catalog, obtained via the TESS satellite. A light curve was constructed and analyzed to determine the times of minimum light, which were then used to build an O-C diagram. The analysis using the Quadratic Polynomial Fitting Method revealed three solutions for the orbital period of V392 Ori. The second condition was calculated from the previous data to the present data. The orbital period was found to be increasing at a rate of 1.21×10^{-3} seconds/year, suggesting ongoing mass transfer and cyclical structural changes in the binary system, as predicted by the TRO theory. Furthermore, periodic variations in the O-C diagram indicate the potential presence of a third body with an orbital radius of about 0.67 AU and a period of approximately 17.95 years. On the other hand, the first condition was computed from all data, while the last solution was computed from data excluding pg and vis. The period change is decreasing at rates of 1.134×10^{-3} and 5.176×10^{-3} seconds/year, respectively. The evolution corresponds to the AML theory. Furthermore, the last solution presented for the third body's behavior is at a distance of 0.47 AU, with an orbital period of around 16.28 years. When considering the observations in modern astronomy, which includes modern instrumental photography, the third condition may show a trustworthy solution. However, this binary should be observed further to study its evolution.

5. Acknowledgements

The author would like to thank the National Aeronautics and Space Administration for the TESS Eclipsing Binary Catalog.

Author Contributions: Conceptualization, methodology, investigation, W.M., formal analysis, writing—original draft preparation, C.W. and W.M.; Observation, T.H., writing—review and editing, and project administration, W.M.

Funding: This research was funded by Thailand Science Research and Innovation (TSRI) through Chiang Mai Rajabhat University, Fiscal Year 2025..

Conflicts of Interest: The authors declare no conflict of interest.

References

- [1] Maithong, W.; Tajumpa, A. Period Change and Third Body Study of a Binary System V781 Tauri. *Udon Thani Rajabhat University Journal of Science and Technology* **2019**, 7(2), 179–187. (in Thai)
- [2] Soonthornthum, B. *Astrophysics*. Chiang Mai University. **2007**. (In Thai)
- [3] SIMBAD Astronomical Database - CDS (Strasbourg). (Accessed 2024, September 22). <http://simbad.u-strasbg.fr/simbad/>
- [4] Liu, X.; Tan, H.-S.; Leung, K. UBV observations of short-period close binary V392 Orionis. *Astrophysics and Space Science* **1988**, 141(1), 21–25. <https://doi.org/10.1007/BF00641912>

- [5] Hong, K.; Lee, J. W.; Koo, J.; Park, J.; Kim, S.; Rittipruk, P.; Kanjanasakul, C.; Han, C. Time-series Spectroscopy of the Oscillating Eclipsing Algol System V392 Orionis. *The Astronomical Journal* **2019**, *157*, 1–8. <https://doi.org/10.3847/1538-3881/aaf39f>
- [6] TESS Eclipsing Binary Catalog. (Accessed 2024, September 22). <http://tessebs.villanova.edu/>
- [7] Ricker, G. R. et al. Transiting Exoplanet Survey Satellite. *Journal of Astronomical Telescopes, Instruments, and Systems* **2015**, *1*(1), 014003-1–10.
- [8] Bob Nelson's Database of Eclipsing Binary O-C Files, AAVSO. (Accessed 2024, October 22). <https://www.aavso.org/bob-nelsons-o-c-files>
- [9] Qian, S. Orbital Period Changes of Contact Binary Systems: Direct Evidence for Thermal Relaxation Oscillation Theory. *Mon. Not. R. Astron. Soc.* **2001**, *328*, 914–924. <https://doi.org/10.1046/j.1365-8711.2001.04921.x>
- [10] Lucy, L. B.; Wilson, R. E. Observational Tests of Theories of Contact Binaries. *The Astrophysical Journal* **1979**, *231*, 502–513. <https://doi.org/10.1086/157212>